

Surface Science Letters

SrTiO₃(001) reconstructions: the (2 × 2) to c(4 × 4) transition

Fabien Silly, David T. Newell, Martin R. Castell *

Department of Materials, University of Oxford, Parks Road, Oxford OX1 3PH, UK

Received 27 March 2006; accepted for publication 23 May 2006

Available online 16 June 2006

Abstract

Scanning tunneling microscopy (STM) is used to investigate the (001) surface structure of Nb doped SrTiO₃ single crystals annealed in ultra high vacuum (UHV). Atomically resolved images of the (2 × 2) reconstructed surface are obtained after annealing a chemically etched sample. With further annealing dotted row domains appear, which coexist with the (2 × 2) reconstruction. The expansion of these domains with further annealing gives rise to the formation of a TiO₂ enriched c(4 × 4) reconstruction.

© 2006 Elsevier B.V. All rights reserved.

Keywords: Scanning tunneling microscopy; Surface relaxation and reconstruction; Alkaline earth metals; Titanium; Surface structure, morphology, roughness, and topography; Low index single crystal surfaces; Surface defects

Strontium titanate has attracted much attention as a model perovskite system. Its bulk, thin film, and small particle structure [1–5], as well as its electronic properties [6–13] have been extensively investigated. SrTiO₃ has been used as a lattice matched substrate for the growth of high temperature superconductors [14,15]. It was also successfully used as a support for metal thin film and nanocrystal growth for Au [16,17], Pd [18–21], Pt [22] Co [23], Cu [24], Ni [25], Fe [26], Mo [27], Ir [28], Cr [29], Ag [30] as well as a support for the formation of TiO_x islands [31–33], Sr [34] and SrO rich islands [35], and perovskite nanodots [36]. Heteroepitaxial growth on SrTiO₃ has highlighted the importance of the nature of the surface. SrTiO₃(001) has the ability to support numerous surface reconstructions. Changes in surface reconstruction can be the key parameter that determines nanocrystal shape, as in the case of Pd [18]. To date the reconstructions reported include (1 × 1), (2 × 1), (2 × 2), c(4 × 2), c(4 × 4), (√5 × √5)R26.6°, (√13 × √13)R37.7°, (6 × 2), c(6 × 2) and (9 × 2) [21,23,1,37–46,34,47–50]. Technological applications of this material require the optimization of the processes that can reproducibly produce a given surface

structure. In this paper, we report on STM studies of the reconstructions of an HF etched SrTiO₃(001) substrate under annealing conditions in UHV. We show that a (2 × 2) reconstruction forms at low temperature. Further annealing gives rise to the appearance of domains of linear structures that coexist with the (2 × 2) reconstruction. We then show that the expansion of these domains with annealing time results in the formation of a c(4 × 4) reconstruction.

SrTiO₃ is a cubic perovskite with a 3.905 Å lattice parameter. In its pure form it has a 3.2 eV band gap which makes it unsuitable for imaging with the scanning tunneling microscope (STM). To overcome this problem we use crystals doped with 0.5% (weight) Nb. These crystals were supplied by PI-KEM, UK, with epi-polished (001) surfaces. SrTiO₃(001) samples were prepared by chemically etching the crystals in a buffered NH₄F–HF solution and introduced into the ultrahigh vacuum (UHV) chamber of a STM (JEOL JSTM4500S) operating at a pressure of 10^{–10} mbar. Etched tungsten tips were used to obtain constant current images at room temperature with a bias voltage applied to the sample. Resistive sample heating in the UHV chamber was achieved by passing a current through the sample. Temperature measurement was performed through a viewport using a disappearing filament optical pyrometer.

* Corresponding author.

E-mail address: martin.castell@materials.ox.ac.uk (M.R. Castell).

Fig. 1 shows the surface of an etched SrTiO₃(001) sample annealed in UHV at 950 °C for 2 h. A high resolution STM image (Fig. 1a) shows a surface with a square lattice reconstruction orientated along the crystallographic axes of the sample. The measured $\langle 100 \rangle$ periodicity along this lattice is 8.0 Å. This corresponds to a (2×2) reconstruction and covers the entire surface of the sample. The irregular dark and bright features on the surface are most likely due to crystal defects such as O vacancies or Nb dopants. The image labeled Fig. 1b shows two step edges on this surface separating three flat terraces. The step edges are wavy and show no preferential crystallographic orientation. The wavy step edges are similar to those of the (2×1) reconstruction, but are unlike the oriented steps reported on the $c(4 \times 2)$ reconstruction [37]. The step heights are

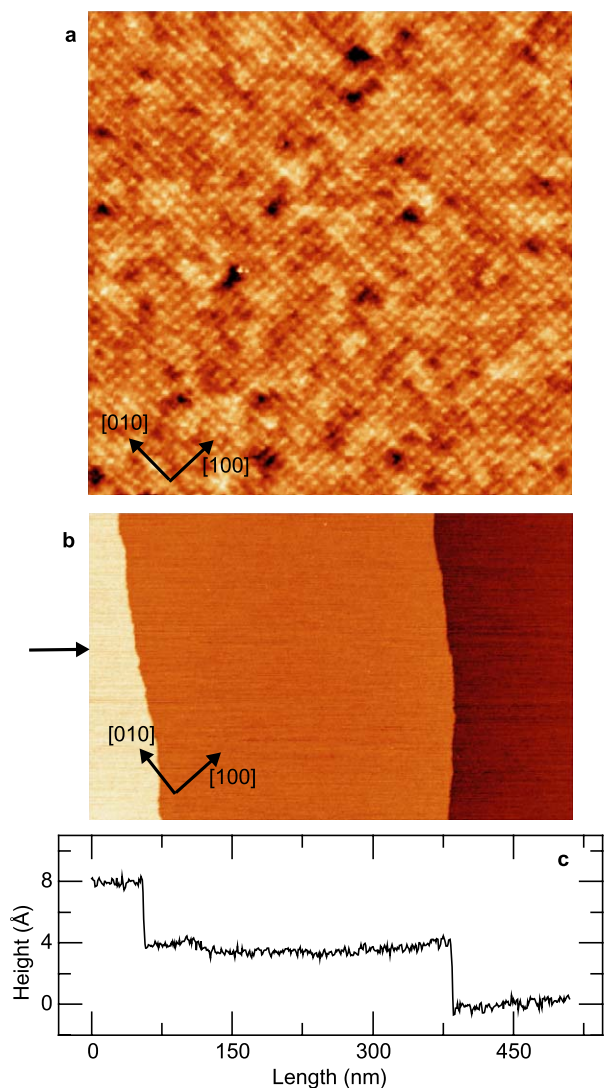


Fig. 1. STM data from the SrTiO₃(001)- (2×2) reconstructed surface. The atomic periodicity is shown in the $35 \times 35 \text{ nm}^2$ image in (a); $V_s = +0.7 \text{ V}$, $I_t = 0.3 \text{ nA}$. In (b) two wavy step edges separating three terraces are shown; $510 \times 325 \text{ nm}^2$, $V_s = +0.8 \text{ V}$, $I_t = 0.3 \text{ nA}$. The black arrow in (b) indicates the position of the height profile shown in (c), which shows that the terrace steps are around 4 Å or one unit cell high.

$3.95 \pm 0.14 \text{ \AA}$ (Fig. 1c), corresponding to one SrTiO₃ unit cell height.

Fig. 2 shows STM images of the SrTiO₃(001) sample after the (2×2) surface was annealed at 1030 °C for 1 h. Fig. 2a shows that domains (bright areas) are now visible on the (2×2) terraces (dark area). An image at higher magnification (Fig. 2b) shows that these domains are composed of lines of bright spots oriented along the $\langle 110 \rangle$ directions. The majority of the visible lines exist as single or double rows of bright spots. The measured periodicity along each row is 11.06 Å which corresponds to the length of the diagonal of the (2×2) surface unit cell. A high resolution image of the junction between the two different domains is presented in Fig. 2c. In this image we see a domain consisting of the dotted row domain on the left, whilst on the right the (2×2) surface reconstruction is atomically resolved. It should be noted that the dotted rows shown in Fig. 2 are

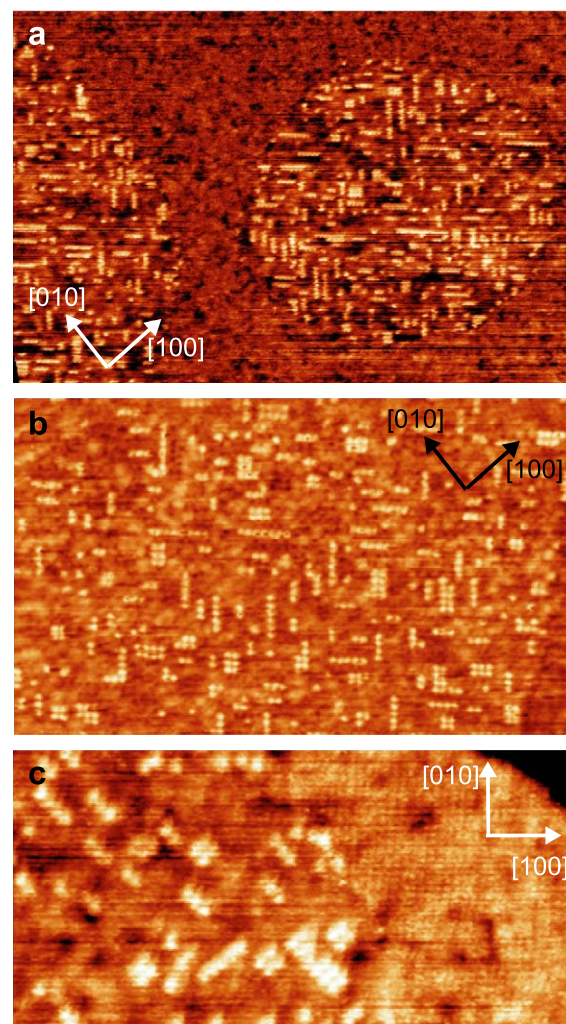


Fig. 2. STM images of dotted row structures on the SrTiO₃(001)- (2×2) surface. In (a) the brighter regions are the dotted row domains; $150 \times 100 \text{ nm}^2$; $V_s = +1.0 \text{ V}$, $I_t = 0.3 \text{ nA}$. The image in (b) shows a dotted row domain in more detail; $85 \times 50 \text{ nm}^2$; $V_s = +1.0 \text{ V}$, $I_t = 0.3 \text{ nA}$. In (c) a dotted row domain and the (2×2) surface are shown; $54 \times 27 \text{ nm}^2$; $V_s = +0.8 \text{ V}$, $I_t = 0.3 \text{ nA}$.

not the same as the nanolines reported in references [41,21] which never appear as single rows and are oriented in the $\langle 100 \rangle$ directions. In Fig. 3 images are shown of the neighbouring dotted row and (2×2) domains. The three images were taken from the same area, but with different imaging conditions. The left hand side of the images is from a dotted row domain, and the smaller triangular patch on the right hand side is a (2×2) domain. At a sample bias voltage of $V_s = +2.0$ V the dotted row domain appears 2.1 Å lower than the neighbouring (2×2) domain (Fig. 3a). At $V_s = +1.0$ V the dotted row domain appears 0.6 Å higher than the (2×2) domain (Fig. 3b). The dotted rows are resolved at $V_s = +1.0$ V, $I_t = 0.3$ nA, and the background of the two domains is of similar height. These observations illustrate the different electronic properties of the dotted row domains and the (2×2) reconstructed domains, although the tunnelling gap resistance dependence as well as the bias voltage dependence should be noted.

Fig. 4 shows the surface of the $\text{SrTiO}_3(001)$ sample after a further anneal in UHV at 1030 °C for 1 h. Imaging with $V_s = +2.0$ V shows a surface that on a large scale image appears disordered and defective, as seen in Fig. 4a. However, when this surface is viewed at higher magnification (Fig. 4b), it can be seen that it is covered by a multitude of small ordered domains consisting of ordered bright spots oriented in the $\langle 110 \rangle$ directions. The measured periodicity along the $\langle 110 \rangle$ directions is 11.15 Å. This is in effect a $c(4 \times 4)$ reconstruction. It is important to note that this reconstruction is not the same as the “brickwork” pattern that evolves from the (2×1) surface and also gives rise to $c(4 \times 4)$ ordering [37]. Fig. 5a and b show STM images of the same area of this surface under two different sample imaging voltages. For $V_s = +1.0$ V, the (2×2) reconstruction is visible (Fig. 5a), whereas at $V_s = +2.0$ V the $c(4 \times 4)$ is seen.

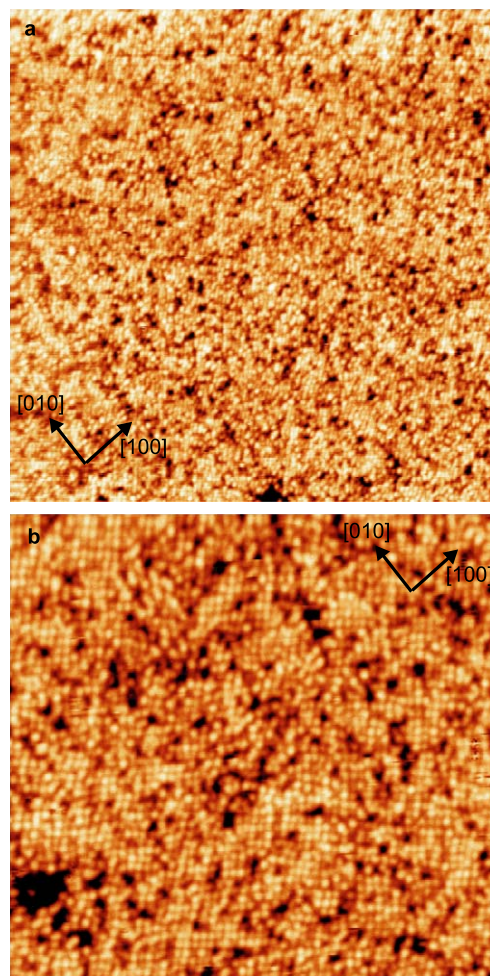


Fig. 4. STM images of the $\text{SrTiO}_3(001)$ - $c(4 \times 4)$ surface. The image in (a) (131×124 nm²) appears to show only disorder, but a higher magnification image in (b) (75×72 nm²) allows local $c(4 \times 4)$ ordering to be resolved. $V_s = +2.0$ V, $I_t = 0.1$ nA.

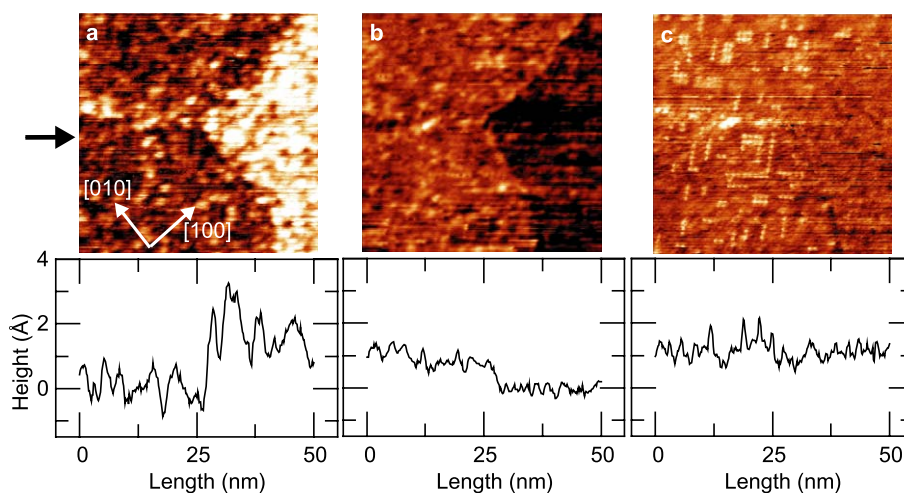


Fig. 3. STM images of the same area of a $\text{SrTiO}_3(001)$ dotted row domain (left) next to a triangular patch of (2×2) (right). The imaging conditions are different for the three figures. Image sizes are 87×81 nm². The (2×2) patch appears bright in (a); $V_s = +2.0$ V, $I_t = 0.1$ nA. It is dark in (b); $V_s = +1.0$ V, $I_t = 0.1$ nA. In (c) there is no contrast; $V_s = +1.0$ V, $I_t = 0.3$ nA.

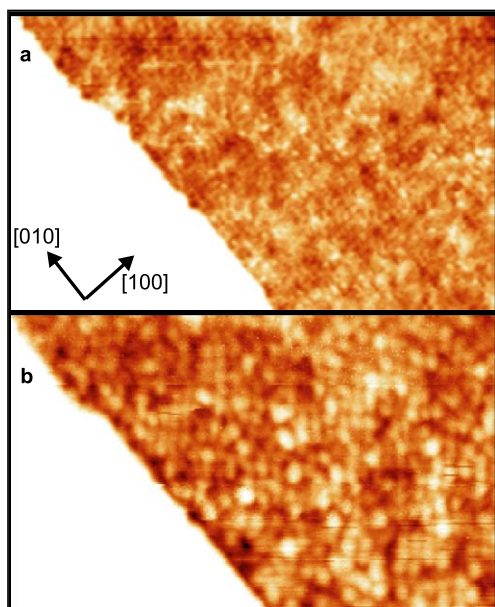


Fig. 5. Bias dependent STM imaging of the surface reconstruction. The images are from the same area, but depending on the voltage either (2×2) order (a) or the $c(4 \times 4)$ reconstruction is seen (b). (a) $\text{SrTiO}_3(001)-(2 \times 2)$, $44 \times 27 \text{ nm}^2$, $V_s = +1.0 \text{ V}$, $I_t = 0.3 \text{ nA}$. (b) $\text{SrTiO}_3(001)-c(4 \times 4)$, $44 \times 27 \text{ nm}^2$, $V_s = +2.0 \text{ V}$, $I_t = 0.3 \text{ nA}$.

To investigate the chemistry associated with the reconstructions we carried out Auger electron spectroscopy (AES) on them and compared the results to a UHV cleavage surface which we take to be representative of SrTiO_3 stoichiometry. The (2×2) reconstruction shows an enhanced Ti signal and reduced O and Sr signals relative to the cleaved sample. AES on the $c(4 \times 4)$ reconstruction shows even further Ti enrichment. No impurity or Nb dopant surface segregation was detected.

This paper shows that prolonged UHV annealing for 2 h at $950 \text{ }^\circ\text{C}$ of an HF etched $\text{SrTiO}_3(001)$ sample gives rise to the formation of a (2×2) reconstruction. On further hotter annealing at $1030 \text{ }^\circ\text{C}$ for an additional hour domains of dotted rows aligned in the $\langle 110 \rangle$ directions form. Further post annealing at $1030 \text{ }^\circ\text{C}$ for another hour gives rise to the formation of $c(4 \times 4)$ domains covering the entire surface of the sample. The periodicity and crystallographic direction of the dotted rows are the same as the bright spots in the $c(4 \times 4)$ domains. This suggests that the $c(4 \times 4)$ domains arise from the growth and ordering of the dotted rows at $1030 \text{ }^\circ\text{C}$. The relative disorder observed in the $c(4 \times 4)$ reconstructed images may arise because of the large number of dotted row domains that nucleate, which in turn will give rise to a high domain junctions density, and thus introduce many defects. The $c(4 \times 4)$ domains or dotted row domains are not visible if the substrate is annealed at low temperatures. These features only appear after extended annealing above $1030 \text{ }^\circ\text{C}$ of a (2×2) surface. The fact that the $c(4 \times 4)$ and the (2×2) ordering can be imaged by STM on the same sample simply by changing the bias values, and that the (2×2) reconstruction exists

before the $c(4 \times 4)$ reconstruction suggests that the dotted rows and the $c(4 \times 4)$ reconstruction grow as an over-layer on the $\text{SrTiO}_3(001)-(2 \times 2)$ surface. It has been shown previously that a different type of nanoline can form on the $\text{SrTiO}_3(001)-c(4 \times 2)$ when annealing above $900 \text{ }^\circ\text{C}$. With annealing temperatures above $975 \text{ }^\circ\text{C}$ full nanoline coverage of the sample surface can be achieved [41,21,51]. The temperature for the growth of these (6×2) and (9×2) reconstructions appears to match the temperature regime reported for dotted row formation in this paper. It is likely that the phenomenon that exists for the $\text{SrTiO}_3(001)-c(4 \times 2)$ surface is also relevant for the $\text{SrTiO}_3(001)-(2 \times 2)$ surface i.e. dotted rows form which eventually give rise to a $c(4 \times 4)$ ad-layer. The AES evidence suggests that the $\text{SrTiO}_3(001)$ (2×2) and $c(4 \times 4)$ reconstructed surfaces are TiO_2 rich, and this has also been confirmed in the case of the nanoline structured surfaces [51]. Moreover, it was observed that Ti and O atoms can diffuse on the $\text{SrTiO}_3(001)$ surface at high temperature to form TiO_2 islands [33]. This evidence indicates that the $c(4 \times 4)$ reconstruction is likely to arise from the formation of a rich TiO_x type ad-layer which grows on the $\text{SrTiO}_3(001)-(2 \times 2)$ surface.

In summary, atomic resolution STM images of the (2×2) and $c(4 \times 4)$ reconstructions on $\text{SrTiO}_3(001)$ surfaces have been shown. The $c(4 \times 4)$ surface is thought to emerge from ordering of dotted row TiO_x rich intermediaries.

Acknowledgment

The authors would like to thank the Royal Society, Oxford Applied Research and DSTL for funding and Chris Spencer (JEOL UK) for valuable technical support.

References

- [1] N. Erdman, K.R. Poepplmeier, M. Asta, O. Warschkow, D.E. Ellis, L.D. Marks, *Nature* 419 (2002) 55.
- [2] Z. Zhang, W. Sigle, F. Phillipp, M. Rühle, *Science* 302 (2003) 848.
- [3] F. Amy, A. Wan, A. Kahn, F.J. Walker, R.A. McKee, *J. Appl. Phys.* 96 (2004) 1601.
- [4] C.L. Jia, A. Thust, K. Urban, *Phys. Rev. Lett.* 95 (2005) 225506.
- [5] G. Cappellini, S. Bouette-Russo, B. Amadon, C. Noguera, F. Finocchi, *J. Phys. Condens. Mat.* 12 (2000) 3671.
- [6] D.W. Reagor, V.Y. Butko, *Nat. Mat.* 4 (2005) 593.
- [7] H. Nyung Lee, H.M. Christen, M.F. Chisholm, C.M. Rouleau, D.H. Lowndes, *Nature* 433 (2005) 395.
- [8] J.H. Haeni, P. Irvin, W. Chang, R. Uecker, P. Reiche, Y.L. Li, S. Choudhury, W. Tian, M.E. Hawley, B. Craigo, A.K. Tagantsev, X.Q. Pan, S.K. Streiffer, L.Q. Chen, S.W. Kirchoefer, J. Levy, D.G. Schlom, *Nature* 430 (2004) 758.
- [9] D.A. Muller, N. Nakagawa, A. Ohtomo, J.L. Grazul, H.Y. Hwang, *Nature* 430 (2004) 657.
- [10] A. Ohtomo, H.Y. Hwang, *Nature* 427 (2004) 423.
- [11] K. van Benthem, G. Tan, L.K. DeNoyer, R.H. French, M. Rühle, *Phys. Rev. Lett.* 93 (2004) 227201.
- [12] D. Kan, T. Terashima, R. Kanda, A. Masuno, K. Tanaka, S. Chu, H. Kan, A. Ishizumi, Y. Kanemitsu, Y. Shimakawa, M. Takano, *Nat. Mat.* 4 (2005) 593.
- [13] R. Shao, M.F. Chisholm, G. Duscher, D.A. Bonnell, *Phys. Rev. Lett.* 956 (2005) 197601.

- [14] R. Sum, H.P. Lang, H.-J. Güntherodt, *Physica C* 242 (1995) 174.
- [15] K. Endo, P. Badica, J. Itoh, *Physica C* 386 (2003) 292.
- [16] F. Silly, M.R. Castell, *Phys. Rev. Lett.* 96 (2006) 086104.
- [17] K. Sun, S. Zhu, R. Fromknecht, G. Linker, L.M. Wang, *Mat. Lett.* 58 (2004) 547.
- [18] F. Silly, M.R. Castell, *Phys. Rev. Lett.* 94 (2005) 046103.
- [19] T. Wagner, G. Richter, M. Rühle, *J. Appl. Phys.* 89 (2001) 2606.
- [20] G. Richter, T. Wagner, *J. Appl. Phys.* 98 (2005) 094908.
- [21] F. Silly, M.R. Castell, *J. Phys. Chem. B* 109 (2005) 12316.
- [22] X. Chen, T. Garrent, S.W. Liu, Y. Lin, Q.Y. Zhang, C. Dong, C.L. Chen, *Surf. Sci.* 542 (2003) L655.
- [23] F. Silly, M.R. Castell, *Appl. Phys. Lett.* 87 (2005) 053106.
- [24] T. Conard, A.-C. Rousseau, L.M. Yu, J. Ghijsen, R. Sporcken, R. Caudano, R.L. Johnson, *Surf. Sci.* 359 (1996) 82.
- [25] D. Vlachos, M. Kamaratos, S.D. Foulis, C. Argiris, G. Borchardt, *Surf. Sci.* 550 (2004) 213.
- [26] F. Silly, M.R. Castell, *Appl. Phys. Lett.* 87 (2005) 063106.
- [27] E. Tchernychova, C. Scheu, T. Wagner, Q. Fu, M. Rühle, *Surf. Sci.* 542 (2003) 33.
- [28] B. Koslowski, R. Notz, P. Ziemann, *Surf. Sci.* 496 (2002) 153.
- [29] Q. Fu, T. Wagner, *Surf. Sci.* 505 (2002) 39.
- [30] F. Silly, M.R. Castell, *Appl. Phys. Lett.* 87 (2005) 213107.
- [31] A. Gunhold, L. Beuermann, M. Frerichs, V. Kempter, K. Gömann, G. Borchardt, W. Maus-Friedrichs, *Surf. Sci.* 523 (2003) 80.
- [32] S.B. Lee, F. Philipp, W. Sigle, M. Rühle, *Ultramicroscopy* 104 (2005) 30.
- [33] F. Silly, M.R. Castell, *Appl. Phys. Lett.* 85 (2004) 3223.
- [34] T. Matsumoto, H. Tanaka, K. Kouguchi, T. Kawai, S. Kawai, *Surf. Sci.* 312 (1994) 21.
- [35] B. Rahmati, J. Fleig, W. Sigle, E. Bischoff, J. Maier, M. Rühle, *Surf. Sci.* 595 (2005) 115.
- [36] D. Ruzmetov, Y. Seo, L.J. Belenky, D.-M. Kim, X. Ke, H. Sun, V. Chandrasekhar, C.-B. Eom, M.S. Rzechowski, X. Pan, *Adv. Mater.* 17 (2005) 2869.
- [37] M.R. Castell, *Surf. Sci.* 505 (2002) 1.
- [38] T. Kubo, H. Nozoye, *Phys. Rev. Lett.* 86 (2001) 1801.
- [39] Q.D. Jiang, J. Zegenhagen, *Surf. Sci.* 425 (1999) 343.
- [40] M. Naito, H. Sato, *Physica C* 229 (1994) 1.
- [41] M.R. Castell, *Surf. Sci.* 516 (2002) 33.
- [42] J.E.T. Andersen, P.J. Moller, *Appl. Phys. Lett.* 56 (1990) 1847.
- [43] T. Nishimura, A. Ikeda, H. Namba, T. Morishita, Y. Kido, *Surf. Sci.* 421 (1999) 273.
- [44] P.J. Moller, S.A. Komolov, E.F. Lazneva, *Surf. Sci.* 425 (1999) 15.
- [45] Q.D. Jiang, J. Zegenhagen, *Surf. Sci.* 338 (1995) L882.
- [46] H. Tanaka, T. Matsumoto, T. Kawai, S. Kawai, *Jpn. J. Appl. Phys.* 32 (1993) 1405.
- [47] H. Tanaka, T. Matsumoto, T. Kawai, S. Kawai, *Surf. Sci.* 318 (1994) 29.
- [48] Q.D. Jiang, J. Zegenhagen, *Surf. Sci.* 367 (1996) L42.
- [49] B. Cord, R. Courths, *Surf. Sci.* 162 (1985) 34.
- [50] V. Vonk, S. Konings, G.J. van Hummel, S. Harkema, H. Graafsma, *Surf. Sci.* 595 (2005) 183.
- [51] D.S. Deak, F. Silly, D.T. Newell, M.R. Castell, *J. Phys. Chem. B* 110 (2006) 9246.